

Biocementation of calcareous sand using soluble calcium derived from calcareous sand

Lu Liu^{1,2} · Hanlong Liu^{1,2,3} · Yang Xiao^{3,4} · Jian Chu⁵ · Peng Xiao³ · Yang Wang³

Received: 24 September 2016 / Accepted: 13 June 2017 / Published online: 25 August 2017
© Springer-Verlag GmbH Germany 2017

Abstract A soil improvement method based on a microbially induced carbonate precipitation (MICP) process has been developed in recent years. In this method, calcium carbonate is precipitated in-situ to act as a cementing agency. Calcium chloride is normally used as the calcium source for the MICP process. The use of calcium chloride causes two problems. The first is chloride is corrosive to concrete, and the second is the cost of calcium chloride is relatively high. An improvement to this method is to use other alternative calcium sources. A method to produce soluble calcium using calcium rich calcareous sand and use it as a calcium source for the MICP process to improve the properties of soil has been proposed in this paper. A comparative study between the effect of MICP treatment using soluble calcium produced from calcareous sand and that using calcium chloride with the same concentration of calcium was carried out. The results from both series of tests showed that with increasing amounts of cementation solutions, the strength and stiffness of the treated calcareous sand increased and the permeability decreased. The

scanning electron microscopy (SEM) and X-ray diffraction analyses revealed that the aragonite crystals with an acicular mineral morphology were formed when the soluble calcium was used, whereas the calcite crystals with a rhombohedral mineral morphology were formed when calcium chloride was used. This study also shows that it is feasible to treat calcareous sand using a MICP method with soluble calcium produced from calcareous sand.

Keywords Calcareous sand · Microbially induced carbonate precipitation (MICP) · Soluble calcium · Strength · Stiffness

Introduction

Calcareous sand is a type of marine sediment that is abundant in low-latitude tropical ocean environments such as in the South China Sea, Red Sea, the Persian Gulf, Hawaiian Islands and coastlines of Australia, India and Saudi Arabia (Murff 1987; McClelland 1988). To mitigate the effect of global warming, coastal shoreline restoration or construction of coastal defense systems become necessary. Due to its particular material composition, particle structure, migration pathway and depositional environment, calcareous sand has different physical mechanical properties with the terrigenous quartz sand (Coop 1990) and needs to be improved too to enhance its mechanical properties. Due to the enormous scale of shorelines, the financial requirement associated with coastal restoration, seawall construction or ground improvement is huge. Thus more economical ground improvement solutions need to be developed.

One promising cost-effective soil improvement method is biocementation through a microbially induced carbonate precipitation (MICP) process. This method utilizes biological metabolic processes to create cementation in situ to improve the mechanical properties of soil (Whiffin et al. 2007; Ivanov and Chu 2008; Van

✉ Hanlong Liu
cehliu@hhu.edu.cn

¹ Key Laboratory of Ministry of Education for Geomechanics and Embankment Engineering, Hohai University, Nanjing, China

² College of Civil and Transportation Engineering, Hohai University, Nanjing, China

³ School of Civil Engineering, Chongqing University, Chongqing, China

⁴ Key Laboratory of New Technology for Construction of Cities in Mountain Area, Chongqing University, Ministry of Education, Chongqing 400045, China

⁵ School of Civil and Environmental Engineering, Nanyang Technological University, Singapore, Singapore

Paassen et al. 2010; DeJong et al. 2011; Cheng et al. 2013; Chu et al. 2013; Martinez et al. 2013; Al Qabany and Soga 2013; Montoya and DeJong 2015; Feng and Montoya 2016; Xiao et al. 2017). In this process the bacteria catalyze the hydrolysis of urea to raise the pH of the system and carbonate is produced. In the presence of dissolved calcium ions, the produced carbonate ions will precipitate and form calcium carbonate crystals to bind the sand grains together. In most of these studies, calcium chloride (CaCl_2) is used as the calcium source. The use of calcium chloride causes two problems. The first is chloride is corrosive to concrete, and the second is the cost of calcium chloride is relatively high. Chloride induces steel corrosion, which is a major cause of concrete degradation. The accumulation of corrosion products (oxides/hydroxides) in the concrete pore space near the steel rebar leads to internal stresses that result in cracking and spalling of the concrete cover, which in turn facilitates the intrusion of aggressive agents, oxygen and humidity, and the next step can be the total loss of the structural integrity (Montemor et al. 2003; Shi et al. 2012). We also need to reduce the cost for the MICP-based method. Therefore, it is necessary to explore alternative calcium sources that can be used for MICP. Cheng et al. (2014) proposed a new application of MICP technology to marine environments by using seawater as the sole calcium resource. But the low calcium concentration of seawater limits the calcification rate, which results in requiring 200 flushes to reach a strength gain of about 300 kPa. Choi et al. (2016) produced calcium from eggshell for the MICP process. This method is promising. However, the source of eggshell is limited.

Calcareous sand is a natural material that is high in calcium content and abundant in the coastal region of China. A method to produce soluble calcium from calcareous sand and use it as a calcium source for the MICP process to improve the mechanical properties of calcareous sand has been developed. This method will not only overcome the problems associated with the use of CaCl_2 , but may also reduce the material costs associated with the use of CaCl_2 . The main purpose of this study is to investigate the effectiveness of using the soluble calcium made from calcareous sand as a calcium resource for biocementation of calcareous sand using the MICP method. A comparative study between calcareous sand treated using soluble calcium produced from calcareous sand and that using calcium chloride with the same calcium concentration was carried out using unconfined compressive strength (UCS) tests, permeability tests, scanning electron microscopy (SEM) and X-ray diffraction (XRD).

Materials and methods

Materials

Calcareous sand used in this study was from the Xisha Islands, South China Sea. Natural calcareous sand grains were washed in

distilled water to remove any salt and residues from the ocean and dried at 60 °C for 48 h. The particle size distribution curve and physical properties of the calcareous sand are presented in Fig. 1 and Table 1, respectively. The scanning electron micrograph (SEM) of calcareous sand with various shapes is shown in Fig. 2. Chemical analysis of calcareous sand using X-ray fluorescence spectroscopy (XRF) reveals that it contains 93.70% of calcium, 2.94% of magnesium, 1.92% of strontium, 0.44% of sodium, 0.34% of phosphorus, 0.29% of sulfur, and 0.17% of aluminum. The mineral content of calcareous sand is mostly aragonite as determined using X-ray diffraction analysis (XRD).

Bacterial

Sporosarcina pasteurii (DSMZ 33), a urea hydrolyzing bacterium, was used for this study to induce CaCO_3 precipitation. The bacteria were cultivated in a medium consisting of 20 g/L yeast extract, 10 g/L NH_4Cl , 12 mg/L $\text{MnCl}_2 \cdot \text{H}_2\text{O}$ and 24 mg/L $\text{NiCl}_2 \cdot 6\text{H}_2\text{O}$, at a pH of 9.0. After aerobically incubating at 30 °C in a shaker at 200 rpm until $\text{OD}_{600} \approx 0.8$, the bacteria were then harvested and centrifuged at $4000 \times g$ for 20 min. Then, the supernatant was removed and replaced with 0.9% NaCl before the bacteria were resuspended. Urease activity of the bacterial suspension was 1.6 mM urea/min.

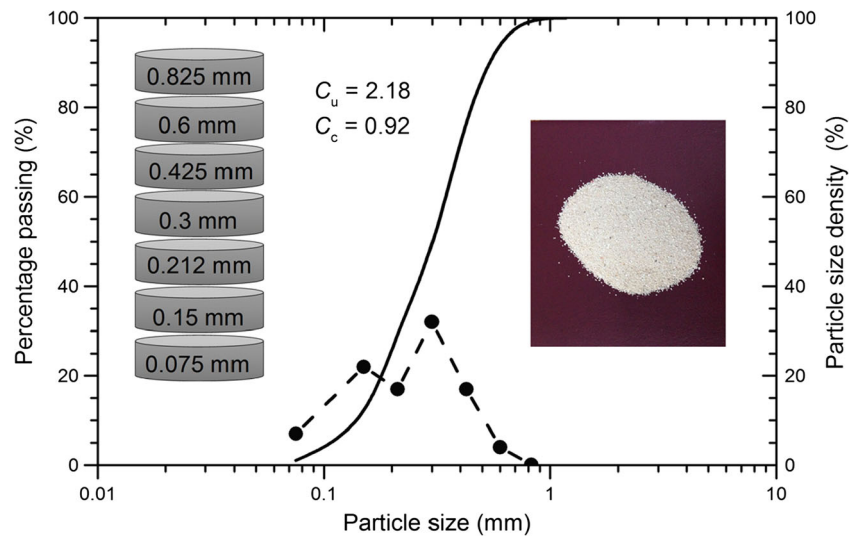
Method to produce soluble calcium from calcareous sand

In this paper, a method to extract calcium ions from calcareous sand in aqueous solutions of acetic acid was adopted. To compare the potential for leaching calcium out from calcareous sand, various acetic acid concentration under varying calcareous sand-to-acetic acid ratios (w/v) were conducted. The pH and calcium ions concentration of the aqueous solutions were measured using a pH meter and the ASTM D511–14 (ASTM 2014) method, respectively. The efficiency was calculated by weighing calcareous sand before and after dissolution.

Sample preparation

First, 150 ml plastic syringes with transparency films (internal diameter 40 mm) were used as test soil columns. Each end of the column was fitted with a layer of approximately 2 cm thick filter gravel and a layer of scouring pad filter. Above the filter layer, the calcareous sand column (40 mm diameter, 2:1 aspect ratio) was prepared by dry pluviation to a relative density of 40%, and then another filter was placed on top of the sample. A peristaltic pump was connected to the top of the column to regulate the flow rate (Fig. 3). To treat calcareous sand specimens, 80 ml bacteria solution was pumped into the specimen at a rate of 40 ml/h and remained in the sand pore space for 6 h to allow the bacterial to attach to the calcareous sand grains. After incubation for 6 h, the excess solution was drained off by gravity. Cementation treatments then began by using the

Fig. 1 Particle size distribution curve of calcareous sand



same pumping rate as in the biological treatment. The cementation solution, which contained a mixture of 1 M Ca^{2+} and 1 M urea, was injected from the top and drained out from the bottom. The drained-out solution was collected and reapplied to the samples two times. The reaction was monitored by measuring calcium concentration of the effluent. To obtain different mechanical properties of the calcareous sand samples, various amounts of cementation solution were pumped into the specimen, as shown in Table 2.

For samples treated using the soluble calcium, the cementation solution was prepared by dissolving calcareous sand in aqueous solutions of 20% acetic acid with a calcareous sand to acetic acid ratio of 1:6 for 24 h (Fig. 4a). The supernatant soluble calcium solution was collected and adjusted for pH to 6.5–7.0 with 20% NaOH solution. After the pH was adjusted, the Ca^{2+} concentration was reduced from 1.2 M to 1.03 M. Then the solution was centrifuged at $4000\times g$ for 20 min to obtain the supernatant (Fig. 4b). The equimolar urea was dissolved into the supernatant to compose the soluble calcium cementation solution of 1 M Ca^{2+} and 1 M urea.

Measuring device and methods

In this experiments, redundant soluble salts were removed from the biocemented samples by flushing with tap water prior to measurements. After biocementation, the MICP-treated samples

were taken out of the molds and any irregularities at the two ends of the samples were trimmed to ensure that they could be uniformly loaded. As the transparency films were smooth, the MICP-treated samples with transparency films could be easily removed from the plastic syringes. The samples were then dried at $60\text{ }^\circ\text{C}$ for 48 h until the mass-loss ratio was less than 0.1% and cooled to room temperature. The oven-dried samples were weighed. With measuring the diameter and length, the dry density could be calculated. Subsequently, all the samples were immersed in tap water for 24 h to characterize the strength, stiffness and permeability properties. Permeability tests on the untreated and biocemented calcareous sand columns were conducted using a falling head method (Proto et al. 2016). Unconfined compression strength (UCS) tests were conducted according to the procedure reported in ASTM D2166 (ASTM 2013) on biocemented specimens with a diameter-to-height ratio of 1:2. The axial load was applied at a constant rate of 1.0 mm/min.

Table 1 Physical properties of calcareous sand

Properties	Values
Specific gravity, G_s	2.75
Mean grain size, D_{50} (mm)	0.32
Coefficient of uniformity, C_u	2.18
Coefficient of curvature, C_c	0.92
Maximum void ratio, e_{\max}	1.75
Minimum void ratio, e_{\min}	1.27

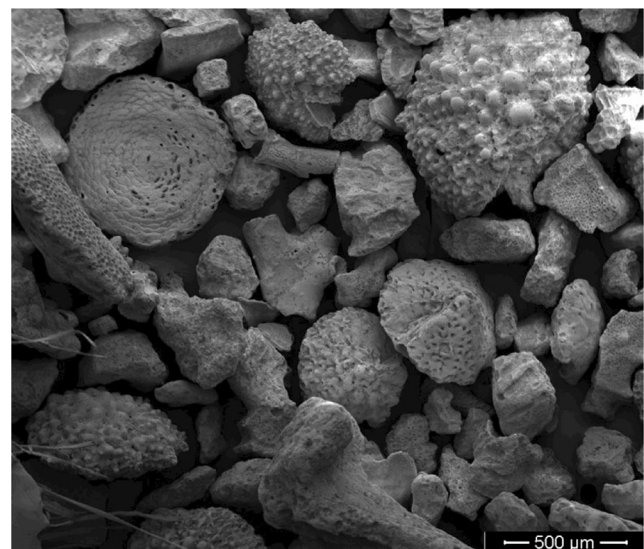


Fig. 2 Scanning electron micrograph of calcareous sand

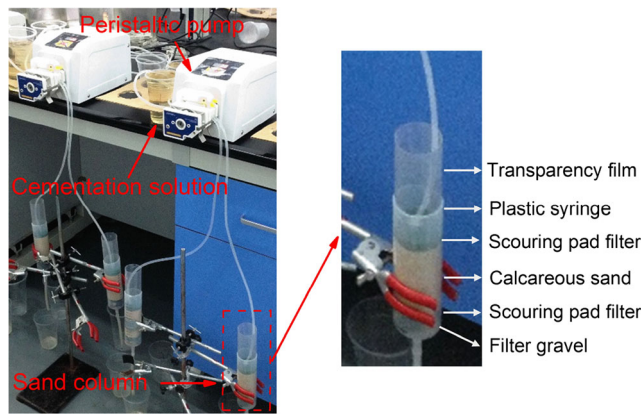


Fig. 3 Experimental apparatus for biocementation of calcareous sand

The mineralogical composition and the morphological structures of the biocementation samples using different calcium sources were analyzed by X-ray diffraction (XRD) and scanning electron microscopy (SEM). After the UCS measurements, the samples were collected and oven-dried at 60 °C for 48 h. Subsequently, a small amount of oven-dried samples were sputter-coated with gold using a KYKY SBC-12 sputter coater prior to the microscopy investigation. A JEOL JSM-7800F field emission scanning electron microscopy (FE-SEM) was conducted on soluble calcium samples and CaCl_2 samples. The samples were crushed using a sterile mortar and pestle and filtered with number 200 mesh prior to XRD analyses. XRD analysis was performed in a Rigaku D/max 2500PC using $\text{CuK}\alpha$. The angle of diffraction (2θ) of the X-ray was set from 10° to 70°, with a step size of 0.02° and a scanning speed of 4°/min.

Results

Soluble calcium from calcareous sand

Dissolution of calcareous sand in different acetic acid concentrations solutions with a calcareous sand to acetic acid ratio of

1:6 are shown in Fig. 5. It can be seen that the concentration of soluble calcium increased with an increase in acetic acid concentration, whereas the increase rate before 20% acetic acid concentration was faster than after 20% acetic acid (Fig. 5a). The pH decreased as the concentration of acetic acid increased, but the effect of acetic acid concentration on the decrease of pH was limited (Fig. 5b). The tendency of dissolving calcareous sand efficiency with different acetic acid concentrations (Fig. 5c) was accordant with the soluble calcium concentration. The pH and soluble calcium concentration changes with time in 20% acetic acid solutions at various calcareous sand-to-acetic acid ratios are shown in Fig. 6. It can be seen that the pH rose quickly at the first half hour and then increased slowly. There was not much difference in the pH between tests with different calcareous sand-to-acetic acid ratios (Fig. 6a). The increasing rate of soluble calcium concentrations also began quickly and then slowed down. The soluble calcium concentration decreased with an increase in sand-to-acid ratio (Fig. 6b). The soluble calcium concentration increased with an increase in acetic acid concentration and decreased with an increase in the sand-to-acid ratio. In practice, the appropriate acetic acid concentration and calcareous sand-to-acetic acid ratio can be selected according to the actual requirement.

Properties of sand treated using the calcium extracted from calcareous sand

Dry density

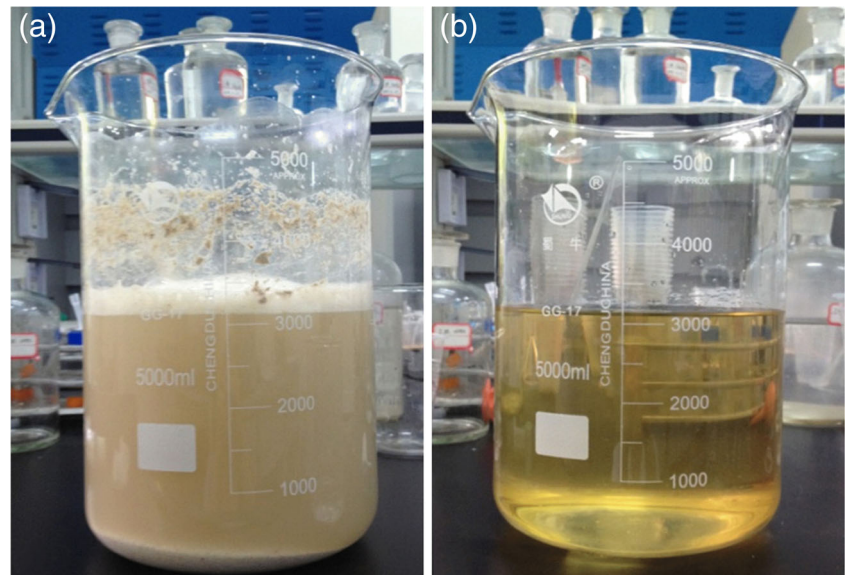
The dry density after biocementation can be used to indicate indirectly the amount of precipitation of calcium carbonate because of the initial densities of the calcareous sand in the molds were essentially the same before being MICP-treated. Fig. 7 shows the variation of dry density with the amount of cementation solutions used for calcareous sand samples treated with different calcium sources and various volumes of cementation solutions. The linear slope of the dry density versus

Table 2 Experimental results

Sample No.	Cementation Recipe	Cementation solutions ^a (L)	Dry density ($\text{g}\cdot\text{cm}^{-3}$)	UCS (MPa)	E_{50} (GPa)
CC1	1 M Calcium Chloride	0.2	1.269	0.208	0.027
CC2	+ 1 M urea	0.3	1.367	0.558	0.053
CC3		0.4	1.489	1.067	0.107
CC4		0.5	1.587	2.300	0.220
SC1	1 M Soluble Calcium	0.2	1.297	0.308	0.042
SC2	+ 1 M urea	0.3	1.415	0.942	0.072
SC3		0.4	1.520	1.467	0.119
SC4		0.5	1.598	2.458	0.213

^aNote: Cementation solution is measured by the volume. The concentrations of all cementation solutions are 1 mol/L. Therefore, the Ca^{2+} content could be determined by the multiplication of the volume and concentration

Fig. 4 Photographs of the soluble calcium produced: (a) during reaction; and (b) after centrifuged



various volumes of cementation solutions suggested that the calcium carbonate precipitation was proportionally increased during injection. Within the same volumes of cementation solution, the dry density of calcareous sand treated with soluble calcium was a little more than that of samples treated with calcium chloride.

Permeability

After the biocementation was finished, permeability was directly measured on each column prior to strength testing. Fig. 8 shows the reductions in permeability with increase in the amounts of cementation solutions for two different calcium sources. As expected, the permeability decreased with increasing cementation solutions. Although the degree of reduction was variable, a large reduction occurred for the soluble calcium-treated samples. The lowest permeability over all samples after treatment was 2.2×10^{-5} m/s compared to the original material permeability of 4.5×10^{-4} m/s, which still retained sufficient permeability and good drainage.

Compressive strength

Fig. 9 shows the unconfined compressive stress-strain behavior of calcareous sand biocemented with calcium carbonate precipitation using soluble calcium and calcium chloride. The tangent Young's modulus at 50% of the peak stress (E_{50}) was determined graphically from the stress-strain curves (van Paassen et al. 2010). From the UCS tests, correlations were established between the amounts of cementation solutions and the values for UCS and E_{50} using soluble calcium and calcium chloride (Figs. 10 and 11). It can be seen that both unconfined compressive strength and stiffness (E_{50}) increased with the increase of cementation solutions for all treated

samples. Both UCS and E_{50} followed exponential relationships with the amounts of cementation solutions, which were in line with previous results reported by van Paassen et al. (2010) and Cheng et al. (2013). It shows that for the same amount of cementation solution, both the strength and stiffness of the samples treated with soluble calcium were higher than those of the control samples treated with calcium chloride. This was in line with the dry density results.

SEM and XRD analyses

The MICP treatment with soluble calcium and calcium chloride showed abundant crystals formed on the surface of the calcareous sand particles and at the contact points between them (Fig. 12). The precipitated crystals of the soluble calcium treated samples were acicular, while the crystals of calcium chloride samples were rhombohedral (probably calcite). The acicular morphology is the typical characteristic of the aragonite. Calcium carbonate exists in three different crystal structures: calcite, aragonite and vaterite. To determine the special crystal structures of the biocementation samples with different calcium sources, X-ray diffraction (XRD) analyses were conducted, as shown in Fig. 13. The XRD patterns show that the crystal structures of the soluble calcium-treated samples was aragonite, while for the calcium chloride-treated samples, the crystal structures were calcite and aragonite. Because the crystal structures of the calcareous sand were aragonite, so the crystal of microbially induced calcium carbonate precipitation using soluble calcium was mainly aragonite and that using calcium chloride was mainly calcite. The XRD analyses prove the acicular and rhombohedral morphologies were the aragonite and calcite, respectively.

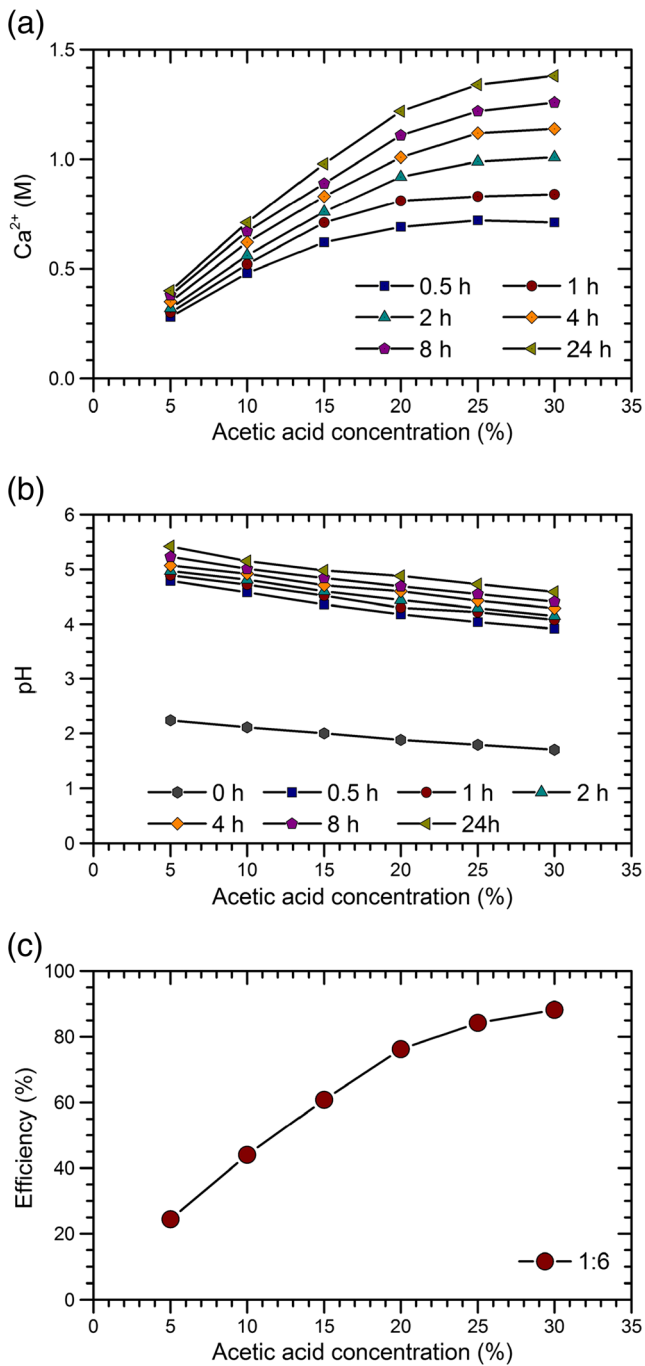


Fig. 5 Dissolution of calcareous sand in different acetic acid concentrations solutions at a calcareous sand-to-acetic acid ratio of 1:6: (a) soluble calcium concentration; (b) pH; (c) efficiency

Discussion

Figs. 14 and 15 show that the UCS and E_{50} plotted against dry density for calcareous sand samples treated with different calcium sources. Correlations were established between the dry density and the values for UCS and E_{50} similar to previous studies (van Paassen 2009). Plotting UCS and E_{50} against dry density showed a better correlation than with the amounts of

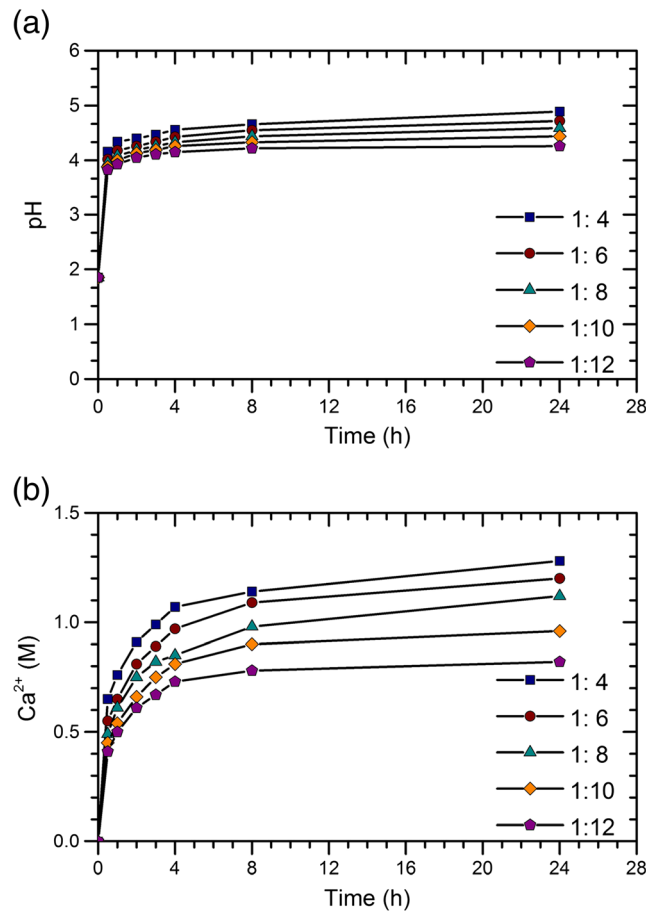


Fig. 6 Dissolution of calcareous sand in an aqueous solution of acetic acid (20%) at various calcareous sand-to-acetic acid ratio: (a) soluble calcium concentration; (b) pH

cementation solutions (Figs. 10 and 11). Higher strength and stiffness for the calcareous sand samples treated with soluble calcium compared to the samples treated with calcium chloride were a result of higher dry density.

When the UCS test results produced in this study were compared with those reported in previous studies, it was found that

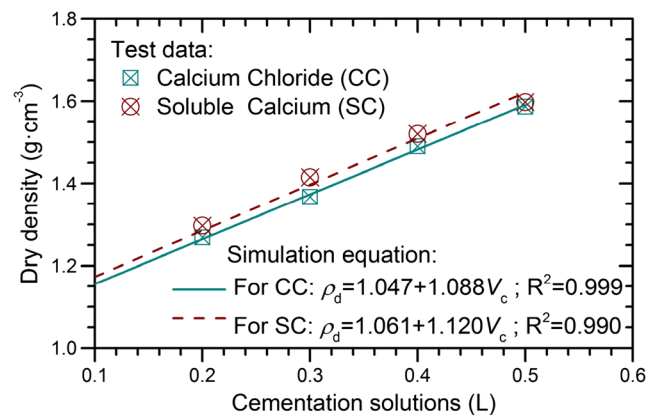


Fig. 7 Variation of dry density with different volumes of cementation solutions for soluble calcium treated samples (SC) and calcium chloride treated samples (CC)

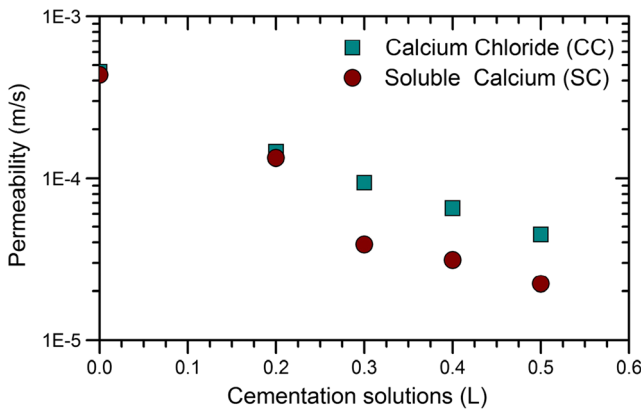


Fig. 8 Variation of permeability with different volumes of cementation solutions for soluble calcium treated samples (SC) and calcium chloride treated samples (CC)

similar patterns of increasing strength were obtained. As shown in Fig. 16, the measured UCS and dry density values with different sands and calcium sources were normalized by the minimum UCS and minimum dry density values, respectively. The normalized UCS values were plotted against the normalized dry

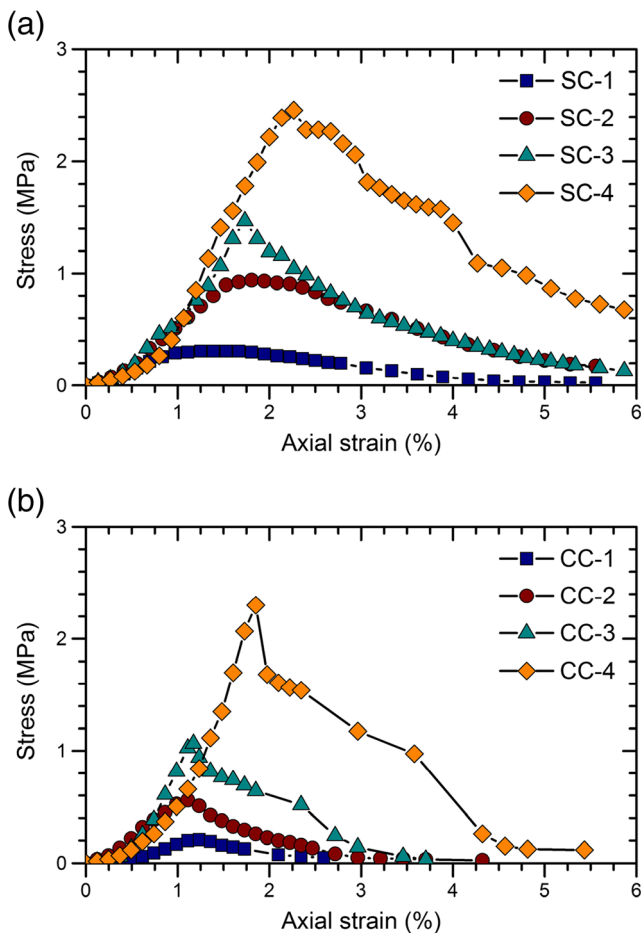


Fig. 9 Unconfined compressive stress-stain behavior of bio cemented calcareous sand using different calcium sources: (a) soluble calcium; (b) calcium chloride

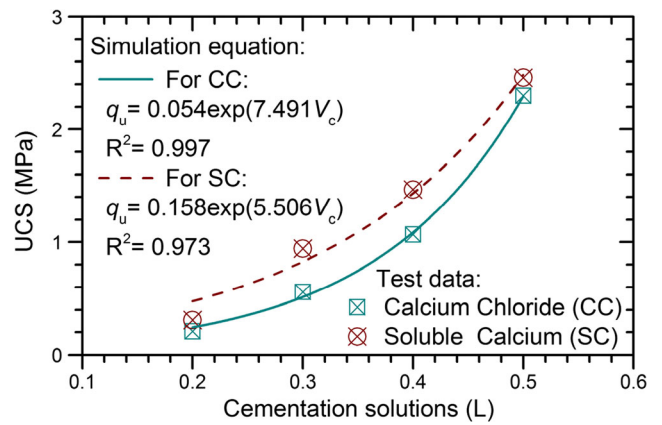


Fig. 10 Variation of unconfined compressive strength (UCS) with different volumes of cementation solutions for soluble calcium treated samples (SC) and calcium chloride treated samples (CC)

density values for MICP-treated samples. Fig. 16 shows that the results of the bio cemented calcareous sand treated with different calcium sources were similar to those produced by van Paassen (2009) who used the same concentration solution (1 M CaCl₂/1 M urea) but different sand (silica sand).

It is of interest to compare the location of bio cemented calcareous sand and MICP-treated silica sand (van Paassen 2009) in terms of the relationship between E_{50} and UCS, as shown in Fig. 17. In Fig. 17, the E_{50} were plotted against the UCS in a double logarithmic space. It can be seen that the E_{50} increased with the increase of the UCS. However, at a similar strength, the stiffness of the bio cemented calcareous sand was lower than that of the silica sand treated by the same concentration solution (van Paassen 2009). The authors believe that this is because the strength (or hardness) of the individual calcareous sand grains caused by the intraparticle pores is lower than that of silica sand.

In Fig. 18, the measured permeability values at different volumes of cementation solutions were normalized with the initial permeability value before the MICP treatment, and the normalized permeability values were plotted against the amount of cementation solutions for bio cemented calcareous

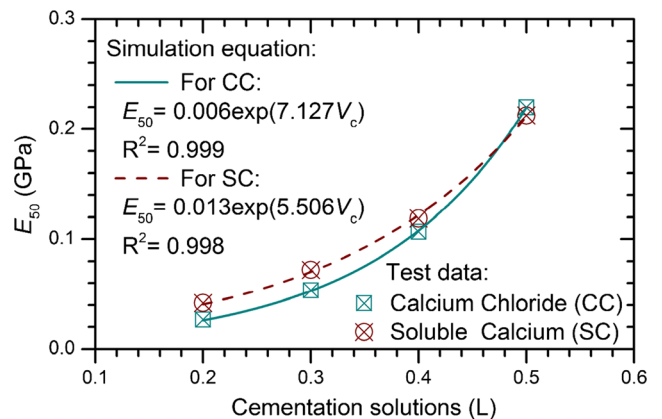
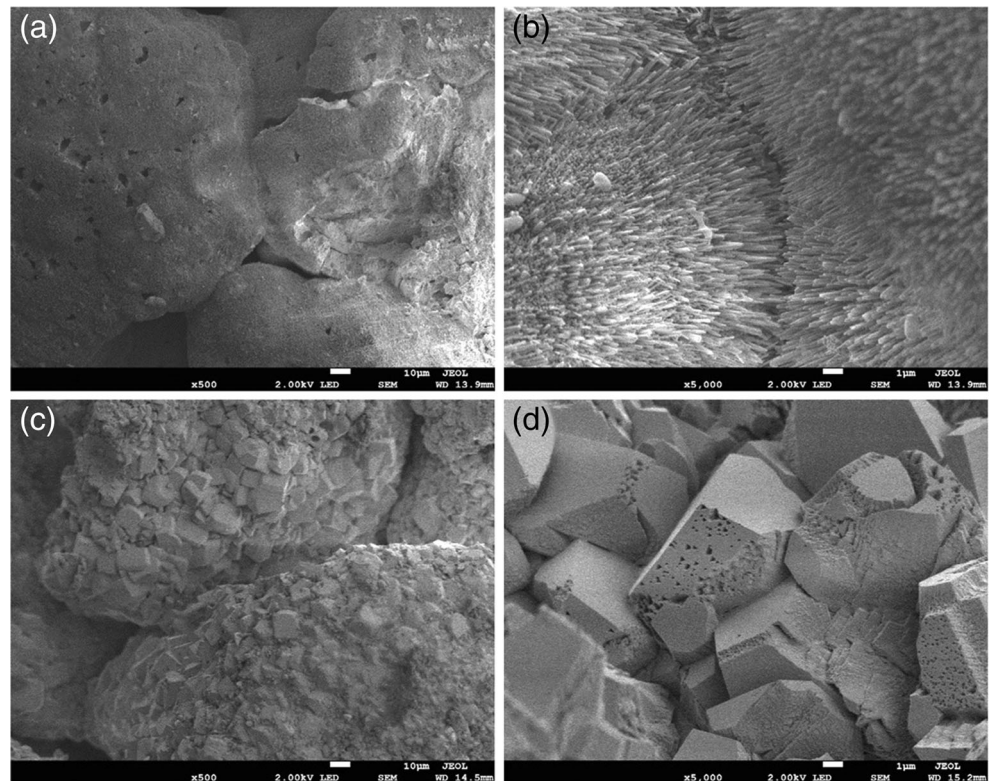


Fig. 11 Variation of Young's modulus (E_{50}) with different volumes of cementation solutions for soluble calcium treated samples (SC) and calcium chloride treated samples (CC)

Fig. 12 Scanning electron microscopy images of biocemented calcareous sand using different calcium sources: (a) soluble calcium; (b) calcium chloride



sand samples with different calcium sources. It can be seen that permeability was reduced to between 5% and 35% of its initial values for all biocemented calcareous sand samples. The degree of reduction in permeability measured in this study was similar to that obtained in previous studies. For example, Al Qabany and Soga (2013) reported 10% to 30% reduction of the initial permeability value using 0.25, 0.5 and 1 M urea-calcium chloride solutions to treat silica sand.

The permeability values obtained from the biocemented calcareous sand samples in this study were compared to permeability values of MICP-treated samples using the same

concentration solution (1 M CaCl_2 /1 M urea) but silica sand (Cheng et al. 2013), as shown in Fig. 19. In the figure, permeability values were plotted against unconfined compressive strength (UCS) for all bio-cemented sand samples. It was found that there were similar patterns of permeability decreasing with increasing unconfined compressive strength. Similar to the previous results (van Paassen 2009; Cheng et al. 2013), it can be seen that, apart from the significant increase in soil strength and stiffness, one advantage of biocementation was attributed to remaining relative high permeability and leaving enough possibilities for further treatment or groundwater flow,

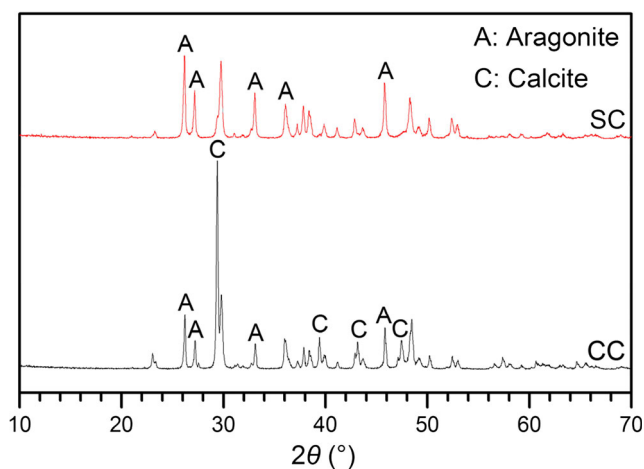


Fig. 13 X-ray diffraction patterns of soluble calcium treated samples (SC) and calcium chloride treated samples (CC)

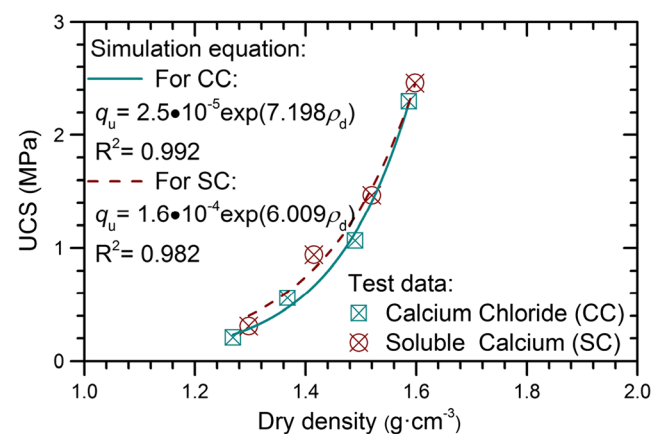


Fig. 14 Variation of unconfined compressive strength (UCS) with dry density for soluble calcium treated samples (SC) and calcium chloride treated samples (CC)

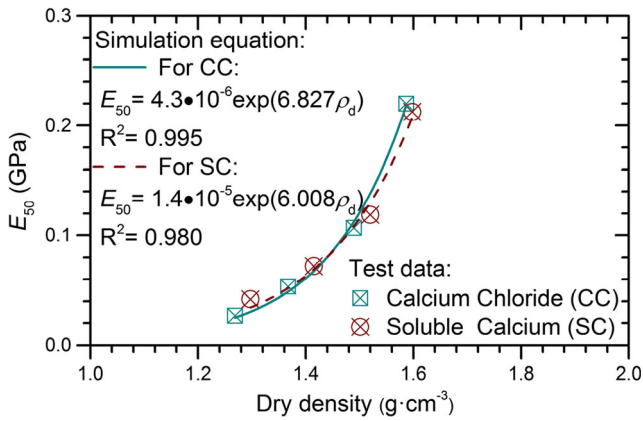


Fig. 15 Variation of Young's modulus (E_{50}) with dry density for soluble calcium treated samples (SC) and calcium chloride treated samples (CC)

compared to the traditional chemical treatment by Portland cement (less than 1×10^{-6} m/s).

MICP is a biogeochemical process that utilizes microbiological methods to mediate the improvement of geological materials used in engineering. A bio-mediated soil improvement system broadly refers to a chemical reaction network that is managed and controlled within soil through biological activity and whose byproducts have the potential to alter the engineering properties of soil. Biocementation is to enhance the strength and stiffness properties of soil through microbial activity or byproducts. (Ivanov and Chu 2008; DeJong et al. 2010, 2013).

Most studies on MICP by urea hydrolysis showed calcite as the predominant mineral phase (Bachmeier et al. 2002; Mitchell and Ferris 2006; DeJong et al. 2011; Cheng et al. 2013; Chu et al. 2013; Montoya and DeJong 2015; Feng and Montoya 2016; Choi et al. 2016). Van Paassen (2009) reported that spherical vaterite is also formed because of a high hydrolysis rate. Vaterite is a thermodynamically unstable crystalline form of calcium carbonate, which tended to transform into the more stable form of calcite (Kralj et al. 1997). Besides, van Paassen (2009) mentioned that calcite growth

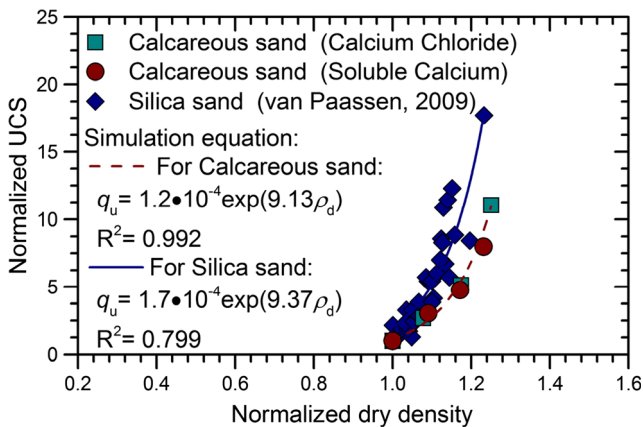


Fig. 16 Normalized unconfined compressive strength (UCS) plotted against normalized dry density for calcareous sand in the present study compared to van Paassen (2009) (silica sand, 1 M CaCl_2 /1 M urea)

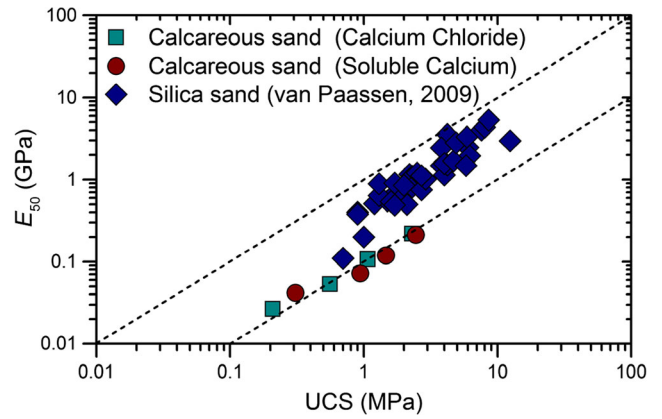


Fig. 17 Young's modulus (E_{50}) plotted against UCS for calcareous sand in the present study compared to van Paassen (2009) (silica sand, 1 M CaCl_2 /1 M urea)

will be more likely after soil is calcareous or has been treated with MICP once before, which explains why calcite was dominant in biocemented calcareous sand using calcium chloride. Furthermore, in the presence of magnesium, aragonite is formed instead of the more stable calcite (Berner 1975). Based on the XRF results, the calcareous sand contains magnesium, so aragonite is formed using the soluble calcium derived from calcareous sand in the MICP process.

This study verified that the soluble calcium derived from calcareous sand could be used as a calcium source for MICP processes to improve the mechanical properties of calcareous sand. Using this method, problems associated with the use of calcium chloride such as corrosion to concrete can be overcome. As calcareous sand is abundant in nature and acetic acid can be produced using a fermentation process of agriculture or vegetation waste, the proposed method will also reduce the cost related to the use of calcium chloride. Therefore, the method proposed will also contribute toward economic sustainability of the construction industry.

In the current study, commercial acetic acid was used for the production of soluble calcium. However, this is not

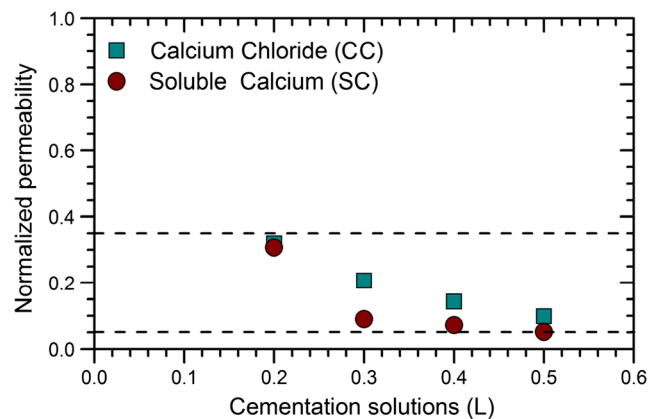


Fig. 18 Decrease in normalized permeability with different volumes of cementation solutions for soluble calcium-treated samples (SC) and calcium chloride-treated samples (CC)

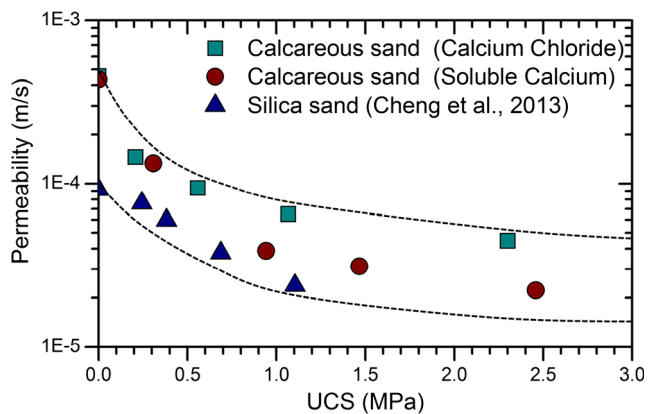


Fig. 19 Permeability plotted against UCS for calcareous sand in the present study compared to Cheng et al. (2013) (silica sand, 1 M CaCl_2 /1 M urea)

necessary, as acetic acid can be produced using agricultural or plantation waste through an acidogenic fermentation process. Soluble calcium with an acidic condition with pH of 5 or above will not affect the activity of the bacteria or the MICP process as shown by previous studies (Fidaleo and Lavecchia 2003; Whiffin 2004). The purpose of this study is to prove that soluble calcium derived from calcareous sand is feasible to be used for MICP-based soil improvement. Further study is underway to establish methods for massive production of soluble calcium from calcareous sand using the more cost-effective acidogenic fermentation process.

Conclusions

This study has demonstrated the feasibility of using soluble calcium produced using calcareous sand as a source of calcium ions for the improvement of calcareous sand using a MICP process. The mechanical properties of calcareous sand treated using soluble calcium were determined and compared with those treated using calcium chloride. The following conclusions can be made:

1. As the amount of cementation solutions increases, the dry density of the calcareous sand treated using either soluble calcium or calcium chloride increases and the permeability decreases.
2. The strength and stiffness of the calcareous sand treated using either soluble calcium or calcium chloride increase exponentially with the increase in cementation solutions, and the samples treated with soluble calcium perform better than those control samples treated with calcium chloride.
3. The SEM and XRD analyses reveal that the precipitated crystals are formed on the surface of the calcareous sand particles and at the contact points between them. These

crystals are mainly aragonite, when soluble calcium is used, or calcite, when calcium chloride is used.

Acknowledgements We would like to acknowledge that this study is supported by the National Natural Science Foundation of China (51578096), the Program of Introducing Talents of Discipline to Universities (B13024) and the Research Innovation Program for College Graduates of Jiangsu Province (KYZZ16_0269).

References

- Al Qabany A, Soga K (2013) Effect of chemical treatment used in MICP on engineering properties of cemented soils. *Géotechnique* 63:331–339
- ASTM (2013) Standard test method for unconfined compressive strength of cohesive soils. ASTM standard D2166, American Society for Testing and Materials, West Conshohocken
- ASTM (2014) Standard test methods for calcium and magnesium in water. ASTM standard D511–14, American Society for Testing and Materials, West Conshohocken
- Bachmeier KL, Williams AE, Warrington JR, Bang SS (2002) Urease activity in microbiologically-induced calcite precipitation. *J Biotechnol* 93:171–181
- Berner RA (1975) The role of magnesium in the crystal growth of calcite and aragonite from sea water. *Geochim Cosmochim Acta* 39:489–504
- Cheng L, Cord-Ruwisch R, Shahin MA (2013) Cementation of sand soil by microbially induced calcite precipitation at various degrees of saturation. *Can Geotech J* 50:81–90
- Cheng L, Shahin MA, Cord-Ruwisch R (2014) Bio-cementation of sandy soil using microbially induced carbonate precipitation for marine environments. *Géotechnique* 64:1010–1013
- Choi SG, Wu S, Chu J (2016) Biocementation for sand using an eggshell as calcium source. *J Geotech Geoenviron Eng* 142:06016010
- Chu J, Ivanov V, Stabnikov V, Li B (2013) Microbial method for construction of an aquaculture pond in sand. *Géotechnique* 63:871–875
- Coop MR (1990) The mechanics of uncemented carbonate sands. *Géotechnique* 40:607–626
- DeJong JT, Mortensen BM, Martinez BC, Nelson DC (2010) Bio-mediated soil improvement. *Ecol Eng* 36:197–210
- DeJong JT, Soga K, Banwart SA, Whalley WR, Ginn TR, Nelson DC, Mortensen BM, Martinez BC, Barkouki T (2011) Soil engineering in vivo: harnessing natural biogeochemical systems for sustainable, multi-functional engineering solutions. *J R Soc Interface* 8:1–15
- DeJong JT, Soga K, Kavazanjian E, Burns S, van Paassen LA et al (2013) Biogeochemical processes and geotechnical applications: progress, opportunities and challenges. *Géotechnique* 63:287–301
- Feng K, Montoya BM (2016) Influence of confinement and cementation level on the behavior of microbial-induced calcite precipitated sands under monotonic drained loading. *J Geotech Geoenviron Eng* 142:04015057
- Fidaleo M, Lavecchia R (2003) Kinetic study of enzymatic urea hydrolysis in the pH range 4–9. *Chem Biochem Eng Q* 17:311–318
- Ivanov V, Chu J (2008) Applications of microorganisms to geotechnical engineering for bioclogging and biocementation of soil in situ. *Rev Environ Sci Biotechnol* 7:139–153
- Kralj D, Brečević L, Kontrec J (1997) Vaterite growth and dissolution in aqueous solution III. Kinetics of transformation. *J Cryst Growth* 177:248–257
- Martinez BC, DeJong JT, Ginn TR, Montoya BM, Barkouki TH, Hunt C, Tanyu B, Major D (2013) Experimental optimization of microbial-induced carbonate precipitation for soil improvement. *J Geotech Geoenviron Eng* 139:587–598

- McClelland B (1988) Calcareous sediments: an engineering enigma. Proceedings of international conference on calcareous sediments, Perth, pp 777–784
- Mitchell AC, Ferris FG (2006) The influence of *Bacillus pasteurii* on the nucleation and growth of calcium carbonate. *Geomicrobiol J* 23: 213–226
- Montemor MF, Simões AMP, Ferreira MGS (2003) Chloride-induced corrosion on reinforcing steel: from the fundamentals to the monitoring techniques. *Cem Concr Compos* 25:491–502
- Montoya BM, DeJong JT (2015) Stress-strain behavior of sands cemented by microbially induced calcite precipitation. *J Geotech Geoenviron Eng* 141:04015019
- Murff JD (1987) Pile capacity in calcareous sands: state of the art. *J Geotech Eng* 113:490–507
- Proto CJ, DeJong JT, Nelson DC (2016) Bio-mediated permeability reduction of saturated sands. *J Geotech Geoenviron Eng* 142: 04016073
- Shi X, Xie N, Fortune K, Gong J (2012) Durability of steel reinforced concrete in chloride environments: an overview. *Constr Build Mater* 30:125–138
- van Paassen LA (2009) Biogrout, ground improvement by microbially induced carbonate precipitation. PhD thesis, Delft University of Technology, the Netherlands
- van Paassen LA, Ghose R, van der Linden TJM, van der Star WRL, van Loosdrecht MCM (2010) Quantifying biomediated ground improvement by ureolysis: large-scale biogrout experiment. *J Geotech Geoenviron Eng* 136:1721–1728
- Whiffin VS (2004) Microbial CaCO_3 precipitation for the production of biocement. PhD Thesis, Murdoch University, Western Australia
- Whiffin VS, van Paassen LA, Harkes MP (2007) Microbial carbonate precipitation as a soil improvement technique. *Geomicrobiol J* 24:417–423
- Xiao Y, He X, Liu H (2017) New lightweight geomaterials: biocemented sand mixed with expanded polystyrene beads. *Sci China Technol Sc*. doi:10.1007/s11431-016-9041-0